



Optics Letters

High-energy ultra-wideband noise-like pulse emitted from a Tm-doped fiber laser

DESHENG ZHAO,^{1,2,†} ZHANXUAN WU,^{1,2,†} XIRAN ZHU,^{3,4} JIAWEI WANG,^{1,2} HAN GAO,^{1,2}
HAOTIAN WANG,^{1,2} LONG TIAN,^{1,2,5} LIRONG CHEN,^{1,2} AND YAOHUI ZHENG^{1,2,*} 

¹State Key Laboratory of Quantum Optics and Quantum Optics Devices, Institute of Opto-Electronics, Shanxi University, Taiyuan 030006, China

²Collaborative Innovation Center of Extreme Optics, Shanxi University, Taiyuan 030006, China

³Beijing Institute of Tracking and Telecommunications Technology, Beijing 100094, China

⁴Science & Technology on Integrated Information System Laboratory, Beijing 100094, China

⁵tianlong@sxu.edu.cn

[†]These authors contributed equally to this work.

*yhzheng@sxu.edu.cn

Received 9 September 2025; revised 8 October 2025; accepted 16 October 2025; posted 16 October 2025; published 28 October 2025

We present a high-energy, ultra-wideband noise-like pulse (NLP) based on nonlinear response and energy enhancements in a 2 μm figure-of-eight fiber laser. The nonlinear response enhancement is achieved by utilizing low-cost commercially available standard communication fiber (SMF-28) and optimizing its length in the figure-of-eight cavity. Enhancing the single-pulse energy of the ultra-wideband NLP is realized by employing a bidirectional pumping scheme. An ultra-wideband NLP with a 3 dB spectrum width of 87.6 nm and a 30 dB spectrum width of 380.1 nm is obtained at an SMF-28 length of 10 m in the nonlinear amplifying loop mirror ring and 300 m in the unidirectional ring. The highest power and pulse energy emitted from the ultra-wideband NLP fiber laser are demonstrated, reaching 429.2 mW and 700.1 nJ, respectively. Such a high-energy ultra-wideband NLP has important application prospects in improving the performance of optical coherence tomography and the flatness of the supercontinuum. © 2025 Optica Publishing Group. All rights, including for text and data mining (TDM), Artificial Intelligence (AI) training, and similar technologies, are reserved.

<https://doi.org/10.1364/OL.578662>

Mode-locking fiber lasers have become an emerging platform for pulse generation due to their flexible and controllable parameters, maintenance-free, compact size, and other advantages [1–3]. Relying on the investigation of mode-locking mechanism as well as the design of cavity structure, fiber lasers have achieved pulsed laser output with different spectral characteristics, which plays an essential part in industrial processing, medical surgery, spectral imaging, and other fields [4,5]. In particular, noise-like pulse (NLP) with ultra-wideband spectrum has unique applications in the supercontinuum generation and optical coherence tomography (OCT), attracting rich research on wideband NLP in the scientific community [6–9]. For example, a wide spectrum NLP containing ultrashort soliton pulses can generate new frequency components more rapidly in obtaining a broader spectrum of the supercontinuum and reduce

the residual pump light component [10]. OCT scanning technique requires wide spectrum pulse as a detection source to realize high quality scanning imaging. A wide spectrum pulse combined with a tunable filter is ideally suited for wavelength-dependent optical fiber sensing.

Wideband NLPs at different wavebands are realized by using different fiber components. In 1 μm waveband, Chen *et al.* achieved wideband NLP with an energy of 255.7 nJ through a cladding pumping scheme combined with a dual nonlinear optical loop mirrors (NOLMs) structure [11]. Lin *et al.* obtained wideband NLP with spectrum range from 1000 to 1160 nm as well as a pulse energy of 35.1 nJ by utilizing a 150 m Hi1060 fiber in the fiber laser [12]. For the research of wideband NLP in 1.5 μm waveband, Sanchez *et al.* designed a Er-Yb co-doped fiber laser with a variable bandwidth tunable filter [13]. The realized NLP has a 3 dB spectrum width of 130.2 nm and a pulse energy of 4.44 nJ. Zhao *et al.* used an appropriate section of highly nonlinear fiber (HNLF) in cavity to obtain an ultra-wideband NLP with a pulse energy of 1.71 nJ [14]. Compared to 1 μm and 1.5 μm wavebands, optical fibers have lower nonlinearity and higher loss in 2 μm waveband, which limits the performance of ultra-wideband NLP. Sobon *et al.* obtained an 2 μm ultra-wideband NLP with a 10 dB spectrum capable of covering 300 nm by using a segment of ultra-high numerical aperture fiber (UHNAF) in the cavity, the maximum pulse energy of NLP is 1.3 nJ [15]. Tong *et al.* acquired a wideband NLP with a pulse energy of 4 nJ and a 10 dB spectral width of 151 nm based on a segment of microfiber with high nonlinearity and large normal dispersion [16]. Zhang *et al.* implemented an NLP with a 3 dB spectrum width of 126 nm and a pulse energy of 0.18 nJ by using UHNAF in cavity [17]. Although ultra-wideband NLP is obtained by using HNLF or UHNAF, the mismatch with the geometrical parameters of the intracavity gain fiber makes the high intracavity loss, the energy is difficult to be effectively boosted. The practical applications have certain requirement on the energy of wide spectrum pulse, such as 2 μm high energy wide spectrum NLP can excite higher frequency conversion efficiency of mid-infrared supercontinuum.

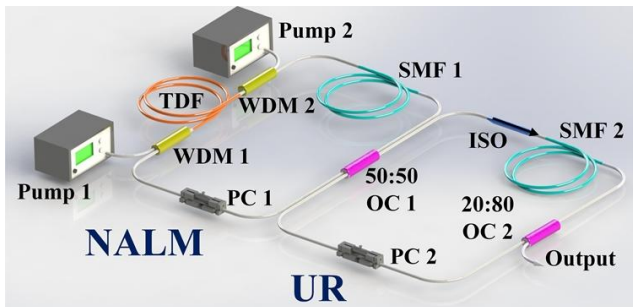


Fig. 1. Experimental set-up of the ultra-wideband NLP fiber laser. WDM: wavelength division multiplexer.

One effective way to enhance the signal-to-noise ratio (SNR) of an OCT system is to increase the energy of the wide spectrum pulse. The pulse energy of wide spectrum pulse is able to be enhanced by the combination of seed and amplification system, but such a solution complicates the system structure. Most of the applications require more compact and simpler wide spectrum pulsed laser generation scheme. An approach is to take advantage of model-locking to output high energy wide spectrum NLPs directly from the fiber laser. However, the energies of the realized ultra-wideband NLPs are still in the lower order of magnitude, there is an absence of technical solution for the direct generation of high-energy, wide spectrum NLP in fiber laser.

Here, it is demonstrated for the first time that ultra-wideband NLP with pulse energy exceeding $0.7 \mu\text{J}$ is generated in a $2 \mu\text{m}$ fiber laser. Using a bidirectional pumping scheme combined with a piece of single-mode fiber (SMF, SMF-28), the fiber laser achieves an ultra-wideband NLP with pulse energy of up to 700.1 nJ and 30 dB bandwidth of 380.1 nm .

Figure 1 illustrates the design scheme of the ultra-wideband NLP fiber laser, consisting of two rings, the nonlinear amplifying loop mirror (NALM) ring and the unidirectional ring (UR). Two home-built Er-Yb co-doped fiber lasers with power of 4.5 W and 4.9 W are served as the pump sources (Pump 1 and Pump 2, centered at 1570.1 nm and 1570.16 nm , respectively). The gain medium is chosen to be a piece of 3.5 m Tm-doped fiber (TDF) with a core diameter of $8 \mu\text{m}$ and a numerical aperture of 0.15 . The UR configuration is ensured for unidirectional propagation of the laser, which is achieved by using an isolator (ISO) in the ring. A 20% port of a $20:80 \text{ OC } 2$ is utilized for output and the other port is employed for intracavity power feedback. In order to provide sufficient nonlinearity in the cavity, two segments of passive fibers (SMF-28, SMF 1 and SMF 2) are inserted into the NALM ring and UR, respectively [18]. Common passive fibers used in $2 \mu\text{m}$ waveband include SMF, SM1950, SM2000, and so on. Compared to other passive fibers, SMF offers lower cost, minimizes splice loss due to its core diameter and numerical aperture matching with the used gain fiber, and provides universal applicability. Two polarization controllers (PCs, PC 1, and PC 2) are used to realize the regulation of the polarization state in the cavity. The whole fiber laser operates at a laboratory temperature of 25°C .

Stable ultra-wideband NLP is obtained by changing the Pump 1 power and PCs, the typical spectrum (measured by the optical spectrum analyzer, AQ6375E) and waveform (characterized by the oscilloscope, RTO64) are depicted in Figs. 2(a) and 2(b). In this case, the SMF 1 length and SMF 2 length

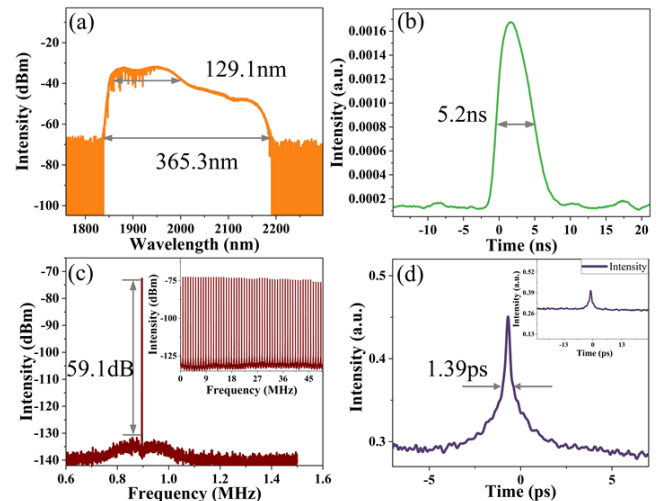


Fig. 2. (a) Pulse spectrum. (b) Pulse waveform. (c) RF spectra of mode-locking pulse. (d) Measured autocorrelation traces.

are 20 m and 195 m , respectively. The spectrum of the mode-locking pulse can cover from 1833.7 nm to 2199.0 nm , with the corresponding spectral covering a range of 365.3 nm . The pulse waveform is exhibited as a Gaussian-like profile with a full width at half maximum (FWHM) of 5.2 ns .

Figure 2(c) exhibits the radio frequency (RF) spectrum (measured by the signal & spectrum analyzer, FSW 8) at different scanning ranges. The repetition frequency of the pulse is 0.895 MHz , which matches the time of one recycle of the pulse in the cavity. The SNR of the pulse is 59.1 dB ($\text{SNR} = I_{\text{peak}} - I_{\text{sub-peak}}$, I_{peak} is the intensity of the signal peak, $I_{\text{sub-peak}}$ is the intensity of the sub-peak), combining with a large range of RF spectrum shows that the NLP has good stability. The operating regime of the fiber laser is distinguishable by measuring the autocorrelation traces (tested by the autocorrelator, APE 50), as presented in Fig. 2(d). The pulse displays a coherent spike on the autocorrelation trace with a FWHM of 1.39 ps . As indicated in the inset of Fig. 2(d), no other interfering signature appears in the wide-range autocorrelation trace and the intensity ratio of the signal to the pedestal is 1.39 , signifying that the obtained pulse is an NLP [19].

The variation of the spectral characteristics of the NLP can be manipulated by changing the parameters of the cavity structure. In particular, the introduction of passive fiber has an important effect on the spectrum of NLP by altering the nonlinear response in the cavity [20]. Thus, the performance of SMF lengths in the NALM ring and UR on the manipulation of the NLP spectrum is comprehensively investigated. Figure 3 exhibits the evolution of the 3 dB and 30 dB spectral widths of the NLP under different SMF lengths. The fiber laser outputs a continuous wave when the length of the SMF 1 is 10 m . The 30 dB spectral bandwidth of the NLP has a maximum of 373.5 nm and a minimum of 45.83 nm , the 3 dB spectral width increases from 15.5 nm to 129.1 nm . It can be seen that enhancing the intracavity nonlinear response to obtain an ultra-wideband NLP requires a reduction of the SMF 1 length as well as an increase of the SMF 2 length. In the NALM ring, increasing the SMF 1 length introduces more nonlinearity and reduces the critical saturation power in the cavity, which allows the NLP to experience pulse broadening effects at lower switching power [21–23]. This results in a lower peak

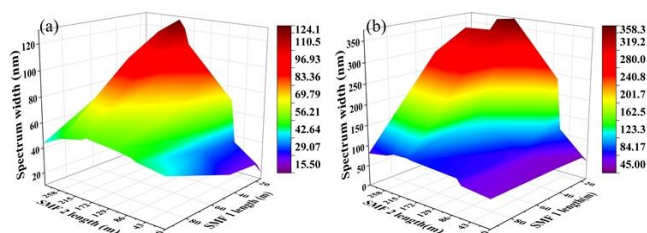


Fig. 3. Effect of different SMF lengths in NALM ring and UR on the (a) 3 dB spectrum width and (b) 30 dB spectrum width of the NLP.

power of the NLP in the cavity and fails to prime more nonlinear effect-induced spectral broadening. The increase of the SMF 2 length induces more nonlinearity while essentially keeps the peak power of the NLP in the NALM ring unchanged, resulting in more nonlinear effect-induced spectral broadening. Therefore, the 30 dB spectral coverage of the NLP decreases as the SMF 1 length increases, and the spectrum of the NLP broadens with the increase of the SMF 2 length.

Following the clarification of the ultra-wideband NLP generation, pulse energy enhancement is investigated, which is achieved by increasing the output power of the fiber laser and decreasing the repetition frequency. Increasing the intracavity passive fiber length reduces the pulse repetition frequency. However, the introduction of higher intracavity losses unavoidably decreases the output power. To this end, the pulse energy of the ultra-wideband NLP with respect to the SMF 1 length in the NALM ring (0–20 m) and SMF 2 length in the UR (100–540 m) is investigated, as shown in Fig. 4(a). It is worth noting that after altering the passive fiber length, self-starting NLP operation cannot be entirely achieved by adjusting the pump power alone. Specifically, longer SMF 2 requires re-adjusting the PCs to achieve NLP mode-locking. Once mode-locking is established through the adjustment of the PCs, turning the pump source on and off again allows stable mode-locking to be achieved without the need to re-establish mode-locking by tapping the fiber or other methods. At a fixed SMF 2 length of 100 m and maximum Pump 1 power, the pulse energy of the NLP increases from 148.7 to 194.4 nJ as the SMF 1 length increases from 0 to 10 m. The nonlinear phase shift difference in the NALM ring determines the formation characteristic of the NLP. The increase in the SMF 1 length decreases the threshold power of the NLP formation, allowing the NLP to have a higher output power at high pump power. This is favorable for the rapid improvement of the pulse energy. However, further increasing the SMF length affects the power loss in the NALM ring. In particular, the establishment of the NLP state requires multiple round-trips of the laser in the cavity. The pulse energy tends to decrease when the effect of power reduction exceeds the effect of increased SMF 1 length on the cavity length. Thus, NLP with peak pulse energy is obtainable at 10 m SMF 1. The pulse energy of the NLP boosts as the length of SMF 2 is changed from 100 to 300 m and the length of SMF 1 remains unchanged. Because the effect of the decrease in repetition frequency exceeds the influence of the power reduction on the pulse energy. For example, the pulse energy of the NLP increases from 221.7 to 378.2 nJ at 10 m SMF 1. Further reduction of the pulse repetition frequency requires longer SMF, which results in the increase of intracavity loss. When the power reduction due to loss is more than the effect of repetition frequency reduction on pulse energy, the pulse energy of the NLP

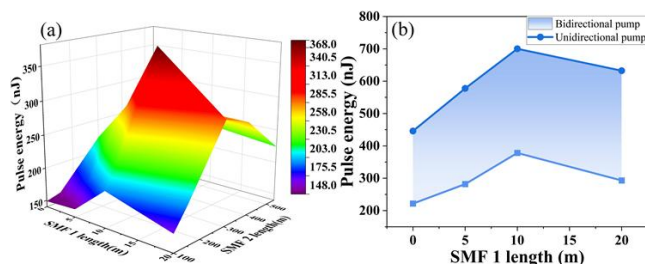


Fig. 4. (a) Effect of different SMF lengths on NLP pulse energy with Pump 1 on. (b) With a fixed SMF 2 length of 300 m, the variation of the pulse energy under different pump schemes and SMF 1 lengths.

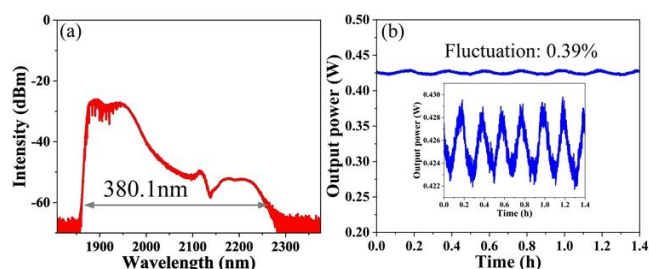


Fig. 5. (a) Spectrum of the ultra-wideband NLP at maximum pulse energy. (b) Power stability over one hour. Inset: zoomed-in details.

decreases as the SMF 2 length increases from 300 to 540 m. Besides the passive fiber length, the coupling ratio of the output coupler significantly affects the spectral width and energy of the NLP. A detailed discussion is provided in Supplement 1.

After Pump 1 reaches the rated maximum power and the power of Pump 2 gradually raises, the power and pulse energy of the ultra-wideband NLP obtains further enhancement. The fiber laser still maintains the single-pulse operation characteristic. Figure 4(b) demonstrates the comparison of NLP energy with different pumping schemes without changing the SMF 2 length. One can see that a higher pulse energy is realized by using a bidirectional pumping scheme, and the maximum pulse energy can reach 0.7 μ J.

The spectrum of the ultra-wideband NLP at the maximum pulse energy is shown in Fig. 5(a). The spectrum expands further into the long wavelengths and the 30 dB spectral width reaches 380.1 nm. The power fluctuation of the NLP over an hour is tested as presented in Fig. 5(b). The fluctuation of the output power is 0.39%, which indicates the good stability of the fiber laser. In general, power stability is dependent on the stability of the mode-locking as well as external environmental disturbance on the fiber laser. When excessive nonlinear effects such as stimulated Raman scattering or modulation instability are present, the stability of the NLP is reduced. In our experiment, a significant increase in intracavity nonlinearity (e.g., SMF-28 length exceeding 540 m) will result in a red shift of the NLP spectral components and generate new sub-pulses in the time domain, which affects the stability of the ultra-wideband NLP. The designed cavity structure employs a long-cavity configuration. By implementing wind shielding, vibration isolation, and active temperature control, power stability can be further enhanced. Besides, the use of non-polarization-maintaining fiber inevitably reduces the fiber laser's immunity to

Table 1. Summary of Typical Ultra-Wideband NLP Fiber Lasers

| Waveband | Mode-Locking | Key Component | Spectrum Width (nm) | Pulse Energy (nJ) | References |
|-------------------|--------------|------------------------|----------------------|-------------------|------------|
| 1 μm | NPR | Hi1060 fiber | 160 (Spectrum range) | 35.1 | [12] |
| 1 μm | NPR | Photonic crystal fiber | 290 (3-dB) | 3 | [24] |
| 1.5 μm | NPR | Filter | 130.2 (3-dB) | 4.44 | [13] |
| 1.5 μm | NPR | HNLF | 203 (3-dB) | 1.71 | [14] |
| 2 μm | NALM | PM1950 | 418.2 (30-dB) | 16.86 | [25] |
| 2 μm | NALM | SMF | 380.1 (30-dB) | 700.1 | This work |

external environmental disturbance. Therefore, adopting an all-polarization-maintaining configuration is useful for improving power stability.

Table 1 exhibits the current typical research on ultra-wideband NLP. With the implementation of SMF-28 for intracavity nonlinear management and bidirectional pumping scheme for energy boosting, the highest-energy ultra-wideband NLP is obtained, and a 41 times energy enhancement is realized compared to the pulse energy of the current 2 μm ultra-wideband NLP.

In summary, we have reported an ultra-wideband NLP with pulse energy exceeding 700 nJ in a 2 μm Tm-doped fiber laser. The highest energy ultra-wideband NLP is achieved through intracavity nonlinear response enhancement and energy boosting. The intracavity nonlinearity management demonstrates that the ultra-wideband NLP fiber laser is favored by using a short passive fiber in the UR. The obtained pulse spectrum is able to cover from 1855.8 to 2300.3 nm, corresponding to a 30 dB spectral width of 380.1 nm. The designed fiber laser can play an important role in supercontinuum, OCT, and so on.

Funding. National Key R&D Program of China (2022YFB3606400); National Natural Science Foundation of China (NSFC) (62225504, U22A6003, 62035015); Fundamental Research Program of Shanxi Province (202403021222033); Scientific and Technological Innovation Programs of Higher Education Institutions in Shanxi (2024L008).

Disclosures. The authors declare no conflicts of interest.

Data availability. Data underlying the results presented in this Letter are not publicly available at this time but may be obtained from the authors upon reasonable request.

Supplemental document. See Supplement 1 for supporting content.

REFERENCES

- Z.-X. Zhang, M. Luo, J.-H. Liu, *et al.*, *Nat. Commun.* **15**, 6148 (2024).
- Z. Wen, Q. Zhang, X. Fan, *et al.*, *Phys. Rev. A: At. Mol. Opt. Phys.* **109**, 033513 (2024).
- J. Zheng, J. Xie, Q. Liu, *et al.*, *Appl. Phys. Lett.* **125**, 051106 (2024).
- B. Cao, C. Gao, K. Liu, *et al.*, *Light Sci. Appl.* **12**, 260 (2023).
- M. Pielach, A. Jamrozik, K. Krupa, *et al.*, *Opt. Express* **32**, 31672 (2024).
- S. Kobtsev and A. Komarov, *J. Opt. Soc. Am. B* **41**, 1116 (2024).
- M. Wang, Q. Gu, F. Yang, *et al.*, *Opt. Express* **32**, 15658 (2024).
- X. Luo, Y. Tang, F. Dong, *et al.*, *J. Lightwave Technol.* **40**, 4855 (2022).
- G. Soboń, *Dissipative Optical Solitons*, M. F. S. Ferreira, ed. (Springer International Publishing, 2022), p 319.
- A. Jose, S. D. Chowdhury, S. Balasubramanian, *et al.*, *Laser Photon. Rev.* **19**, 2400511 (2025).
- H. Chen, S. Chen, Z. Jiang, *et al.*, *Opt. Lett.* **40**, 5490 (2015).
- W.-C. Chang, J.-H. Lin, T.-Y. Liao, *et al.*, *Opt. Express* **26**, 31808 (2018).
- Y. Meng, O. Ougrige, F. Bessin, *et al.*, *Appl. Phys. Lett.* **124**, 201104 (2024).
- X. Wang, A. Komarov, M. Klimczak, *et al.*, *Opt. Express* **27**, 24147 (2019).
- G. Sobon, J. Sotor, T. Martynkien, *et al.*, *Opt. Express* **24**, 6156 (2016).
- Y. Li, Y. Kang, X. Guo, *et al.*, *Opt. Lett.* **45**, 1583 (2020).
- J. Liu, X. Li, S. Zhang, *et al.*, *Opt. Laser Technol.* **148**, 107716 (2022).
- X. Hu, J. Guo, J. Wang, *et al.*, *Light Sci. Appl.* **12**, 38 (2023).
- S. Wang, L. Li, Y.-F. Song, *et al.*, *Front. Inf. Technol. Electron. Eng.* **22**, 318 (2021).
- A. Komarov, K. Komarov, D. Meshcheriakov, *et al.*, *J. Opt. Soc. Am. B* **38**, 961 (2021).
- O. Pottiez, R. Grajales-Coutiño, B. Ibarra-Escamilla, *et al.*, *Appl. Opt.* **50**, E24 (2011).
- Y. Zhou, X. Chu, Y. Qian, *et al.*, *Opt. Express* **30**, 35041 (2022).
- J. Zhao, L. Li, L. Zhao, *et al.*, *Photon. Res.* **7**, 332 (2019).
- X. Li, S. Zhang, J. Liu, *et al.*, *J. Lightwave Technol.* **38**, 3769 (2020).
- D. Zhao, X. Zhu, Z. Wu, *et al.*, *J. Lightwave Technol.* **43**, 5843 (2025).